Blueschist from the Toudaoqiao Area, Inner Mongolia, NE China: Evidence for the Suture between the Ergun and the Xing'an Blocks

Limin Zhao [ID]*[1], **Akira Takasu**[2], **Yongjiang Liu**[1], **Weimin Li**[1]

1. *College of Earth Sciences, Jilin University, Changchun* 130061, *China*
2. *Department of Geoscience, Shimane University, Matsue* 690-8504, *Japan*

[ID]Limin Zhao: http://orcid.org/0000-0003-0495-9377

ABSTRACT: Blueschist accompanied by pelitic schist expose along the Xinlin-Xiguitu fault in the Toudaoqiao area, northeastern China. In this paper, the blueschist is systematically studied on the petrography and mineral chemistry. The amphiboles in the blueschist are zoned from winchite core to magnesioriebeckite/glaucophane rim to winchite outermost rim. The peak metamorphic conditions are defined by the mineral assemblage of magnesioriebeckite/glaucophane, epidote, high-Si phengite (Si<7.1), chlorite, albite, hematite and quartz, indicating an epidote-blueschist facies metamorphism. The *P-T* conditions are estimated as *T*=350–400 °C and *P*=10–12 kbar. The occurrence of the blueschist along the Xinlin-Xiguitu fault strongly suggests the fault is the suture between the Ergun and the Xing'an blocks situated in the eastern portions of the Central Asia orogenic belt (CAOB).
KEY WORDS: Toudaoqiao blueschists, zoned amphibole, *P-T* path, Xinlin-Xiguitu suture.

0 INTRODUCTION

Blueschist is metamorphosed at high *P/T* geothermal conditions, and such conditions are attained along the subduction zone, where relatively old and cold oceanic plate is subducted. Accordingly the presence of blueschist becomes an evidence of terrane boundary (Maruyama et al., 1996; Miyashiro, 1961).

The Toudaoqiao blueschist is located in the northern part of the Xing'an Block, NE China, and the eastern parts of the CAOB (Fig. 1; Sengör et al., 1993). These blueschists have been first described as albite-chlorite-glaucophane schist and glaucophane-albite-epidote-chlorite schist, together with chlorite-quartz schist by Mo (1980). Subsequently, Ye et al. (1994) described these blueschists are high *P/T* metamorphic rocks according to the mineral assemblage. Recently, Zhou et al. (2015) and Miao et al. (2015) newly obtained the ages of 510 and 516±11 Ma for the protolith of the Toudaoqiao blueschist respectively. Zhou et al. (2015) described the Toudaoqiao blueschist comprises a mineral assemblage of glaucophane+epidote+albite+chlorite+muscovite±quartz; Miao et al. (2015) also described the similar mineral assemblage of sodic amphibole+chlorite+epidote+albite+phengite±apatite±quartz, which underwent the peak metamorphic conditions of about 7 kbar and 450–480 °C.

The Toudaoqiao blueschist occurs along the Xinlin-Xiguitu fault in the northern part of the Xing'an Block (Fig. 1). As known that, the boundary between the Ergun Block and Xing'an Block, is a controversy for a long time. The suture locality, tectonic history and closure time of the two blocks are not clear yet.

Although, the blueschist exposed in the Toudaoqiao area has been previously studied on geochronology and petrography, the precise *P-T* path of the blueschist is urgently required; however it is not clear so far. In this paper we petrographically describe the blueschist and related metamorphic rocks, examine the chemical composition of the constituent minerals, with aims of: (1) constructing the *P-T* path of the Toudaoqiao metamorphic rocks and (2) discussing the boundary location, tectonic history and closure time of the Ergun and Xing'an blocks. These results will contribute to better understand the tectonic significance of the eastern portion of the CAOB.

1 GEOLOGICAL OUTLINE OF THE TOUDAOQIAO AREA

Northeast China and adjacent regions form a part of the central east Asia, tectonically located among the Siberian, North China and Pacific plates. This area consists of a collage of micro-continental blocks, e.g., Ergun Block, Xing'an Block, Songnen Block and Jiamusi Block, separating by the Derbugan suture, Xinlin-Xiguitu suture, Heihe-Nenjiang-Hegenshan suture and Mudanjiang fault, respectively (Fig. 1; Zhao et al., 2016; Chen et al., 2009; Xiao et al., 2009, 2003; Miao et al., 2007; Peng et al., 2002; Zhang et al., 1998).

The Ergun Block is located in the northern part of the NE

*Corresponding author: zhaolimin@jlu.edu.cn

China, consists of Meso-Neoproterozoic granitoids and Paleozoic strata, granite and basalt along with Mesozoic volcanic and sedimentary rocks (Wu et al., 2011; Zhou et al., 2011; Ge et al., 2007a, b, 2005; HBGMR, 1993). The Xing'an Block is located in the southeastern part of the Ergun Block, consists of Neoproterozoic and Paleozoic strata, granitoids, metabasalt and gneiss with huge amount of Mesozoic volcanic and granitic rocks and sedimentary rocks (Zhang et al., 2008; Miao et al., 2007, 2003). The Songnen Block is in the central part of the NE China, composes mainly of Songliao Basin, Zhangguangcai Range and the Lesser Xing'an Range. The basement of the Songliao Basin is weakly metamorphosed, the cover sedimentary is only Paleozoic strata, and a few Proterozoic granitoids, according to the drill holes data (Gao et al., 2007; Wang et al., 2006; Wu et al., 2001). The Jiamusi Block consists mainly of Mashan complex, Heilongjiang complex and Early Paleozoic granitic intrusions. The Mashan complex is related to the Early Paleozoic metamorphic event; the Heilongjiang complex consists mainly of blueschist, ultra-mafic rocks, metamorphosed pillow lava and marbles (Wilde et al., 2003, 1997).

Toudaoqiao blueschist occurs along the Xinlin-Xiguitu suture in the northern part of the Xing'an Block (Fig. 1). As known, the boundary between the Ergun Block and Xing'an Block, is a controversy for a long time. There are mainly two models (Fig. 1b). One is that the Derbugan fault is the boundary.

There is clear geophysical evidence showing the different characteristic gravity anomalies between the east side and west side of the Derbugan fault (HBGMR, 1981), but there are no occurrence of ophiolite or blueschists. The other model is that Xinlin-Xiguitu suture is the boundary, which is distinguished by the Xinlin ophiolite, in the eastern part of the suture (Li, 1991), and Toudaoqiao blueschist in the northwest part of the Xing'an Block.

The outcrop in the Toudaoqiao area is very poor and covered with heavy forest. It consists mainly of Neoproterozoic to Paleozoic strata, Late Paleozoic and Mesozoic granites together with huge amounts of Mesozoic acidic to basic volcanic rocks and mélange (Fig. 1c; HBGMR, 1981). The mélange is composed of blocks of Ordovician, Lower Devonian and Lower Carboniferous breccias. Blueschist accompanied by pelitic schist occur to the south of the Toudaoqiao Village, all the metamorphic rocks have a NE-SW trend (HBGMR, 1981). The blueschist and associated metamorphic rocks are bounded by Jurassic volcanic rocks to the northwest with a high angle fault contact, and to the southeast they are covered by Quarternary deposits.

Three samples of blueschist (TD7, TD9 and TD13) and one sample of pelitic schist (TD6) were collected for this study (Fig. 1c).
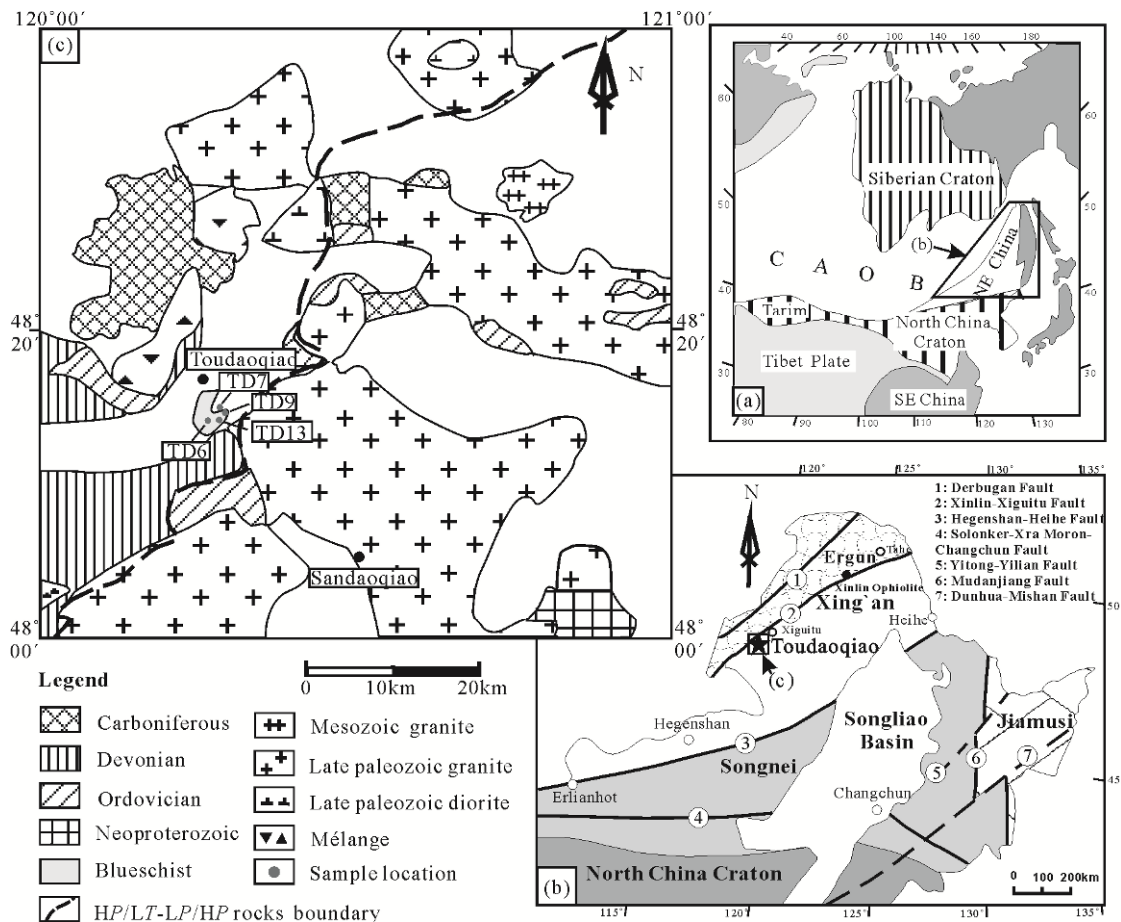

Figure 1. Simplified geological maps of the study area. (a) Geotectonic map of the eastern Asia (Wu et al., 2007); (b) Geological map of NE China showing the main continental blocks, boundary suture and faults (after Wu et al., 2007); The location of study area is shown by solid star and the location of Xinlin ophiolite is shown by solid circle; (c) Geological map of the Toudaoqiao area (after Heilongjiang Bureau of Geology and Mineral Resources, HBGMR, 1981).

2 PETROGRAPHY OF BLUESCHISTS AND PELITIC SCHISTS

Blueschist sample TD13 consists mainly of amphiboles (sodic and sodic-calcic amphiboles) (20%–25%), epidote (10%–15%), phengite (5%), chlorite (30%–35%), albite (15%) and quartz (5%) (Fig. 2a). Titanite, hematite, calcite and apatite are present as accessory minerals. Schistosity is defined by prefered orientation of amphibole and chlorite. Amphibole occurs as subhedral prismatic crystal with size up to 0.5 mm long. It contains inclusions of epidote, chlorite, titanite, rutile and hematite (Fig. 2e). It is partly replaced by chlorite along the rim and crack (Figs. 2e and 2g). Some amphiboles are optical zoned with winchite core, magnesioriebeckite/glaucophane rim and winchite outermost rim (Fig. 2a). Phengite appears as anhedral platy crystal up to 0.2 mm long. Epidote occurs as anhedral rounded grain with size up to 0.1 mm across. Chlorite is euhedral to subhedral, with size up to 0.3 mm across. Albite is subhedral to anhedral, and its size is up to 0.5 mm across.

Blueschist sample TD7 consists mainly of amphibole (sodic and sodic-calcic amphiboles) (10%–15%), epidote (10%–15%), albite (10%), phengite (5%), chlorite (35%–40%), quartz (5%), calcite and titanite with minor amounts of hematite. Amphibole occurs as subhedral prismatic crystal with size up to 0.2 mm long. It contains inclusions of amphibole (kataphorite and barroisite) as a relic of the precusor metamorphic event. Some amphiboles are optical zoned with winchite core to magnesioriebeckite rim, accasionally with winchite outermost rim (Fig. 2b).

Blueschist sample TD9 consists mainly of chlorite (20%–25%), epidote (5%–10%), amphibole (sodic amphibole) (10%–15%), quartz (5%), albite (35%–40%), hematite, apatite and titanite. Amphibole occurs as euhedral prismatic crystal with size up to 0.3 mm long. Epidote occurs as anhedral rounded grain with size up to 0.1 mm across. Chlorite is euhedral to subhedral, and its size is up to 0.3 mm across (Fig. 2c).

Pelitic schist sample TD6 consists mainly of phengite (20%–25%), albite (5%), chlorite (25%–30%) and quartz (35%–40%). Hematite, calcite, apatite and carbonaceous material are present as accessory minerals. Schistosity is defined by phengite and chlorite. Phengite occurs as anhedral platy crystal up to 0.3 mm long. Chlorite is subhedral, with size up to 0.4 mm across. Albite is subhedral to anhedral, and its size is up to 0.5 mm across (Fig. 2d).

3 MINERAL CHEMISTRY

The chemical compositions of minerals were analyzed using a JEOL JXA-8800 electron microprobe analyzer at the department of Geoscience, Shimane University. The analytical conditions were as follows: accelerating voltage, 15 kV; probe current, 2×10^{-8} A; and probe diameter, 5 μm. The representative mineral chemical compositions are shown in Table 1. Abbreviations of the minerals and end-members used in the figures and tables are followed Kretz (1983).

3.1 Amphibole

For Fe^{3+} estimation of the amphibole, a normalization factor of 13eCNK (O=23) was used, and the classification of amphibole was referred from Leake et al. (1997).

Amphiboles are classified as magnesioriebeckite, winchite and a little amount of glaucophane (Figs. 3a and 3c). Magnesioriebeckites are found in the matrix of each blueschist samples and rims of the zoning amphiboles, winchites are found in the core and outermost rim of sample TD13 and TD7, glaucophanes are found in sample TD13 and TD9. Amphiboles in blueschist sample TD7 and TD13 are commonly zoned with winchite core and magnesioriebeckite/glaucophane rim (Fig. 2e), occasionally accompanied by outermost rim of winchite (Figs. 2f–2h). The cores of the zoned amphiboles have compositions of winchite with Si=7.50–7.83 apfu, Na_B=0.55–1.46 apfu, Al^{VI}=0.13–0.56 apfu, $X_{Mg}[=Mg/(Mg+Fe^{2+})]$ =0.55–0.95, the rims have compositions of magnesioriebeckite and glaucophane with Si=7.83–7.96 apfu, Na_B=1.52–1.79 apfu, Al^{VI}=0.20–0.94 apfu, X_{Mg}=0.54–0.64, the outermost rims have compositions of Si=7.83–7.92 apfu, Na_B=0.80–1.49 apfu, Al^{VI}=0.09–0.40 apfu, X_{Mg}=0.61–0.62. The Si content in the zoned amphiboles of sample TD13 shows a little increase, then decrease, Na_B content shows dramatic increase, then decrease, Al^{VI} content shows dramatic increase, then decrease, X_{Mg} is continuous from core to outermost rim (Fig. 3b).

3.2 Phengite

Phengites in blueschist sample TD13 have high Si contents ranging from 6.67 to 6.98 apfu (O=22), and $X_{Na}[=Na/(Na+K)]$ ranging from 0.010 to 0.038, (Fe+Mg) contents ranging from 1.29 to 1.74 apfu. Phengites in blueschist sample TD7 have a little higher Si contents (6.78 to 7.09 apfu) than those in sample TD13, X_{Na} ranges from 0.01 to 0.042, and (Fe+Mg) contents ranges from 1.25 to 1.70 apfu. Phengites in pelitic schist also have high Si contents ranging from 6.68 to 6.93 apfu, and X_{Na} ranging from 0.002 to 0.039, (Fe+Mg) contents ranging from 1.09 to 1.70 apfu (Fig. 3d).

3.3 Epidote

Epidotes are commonly homogeneous, X_{Ps}=$Fe^{3+}/(Al+Fe^{3+})$ ranges from 0.31 to 0.35. Some zoned epidotes show X_{Ps} slightly decreasing from core to rim.

3.4 Chlorite

Chlorites in blueschist are characterized by compositions with Si contents ranging from 5.46 to 6.36 apfu and $X_{Mg}[=Mg/(Mg+Fe^{2+})]$ of 0.38–0.45. Chlorites in pelitic schist have compositions with Si contents ranging from 5.56 to 6.03 apfu and X_{Mg} of 0.49–0.52.

4 MINERAL PARAGENESIS AND *P-T* ESTIMATIONS
4.1 *P-T* Estimation for the Blueschist Sample TD13

Based on the texture and chemical compositions of the constituent minerals, the metamorphism of the blueschist sample TD13 is divided into three stages, i.e., the prograde, peak and retrograde stages. The *P-T* evolution of blueschist is constructed from the zoned amphiboles that show zoning from winchite core to magnesioriebeckite/glaucophane rim, then winchite outermost rim.
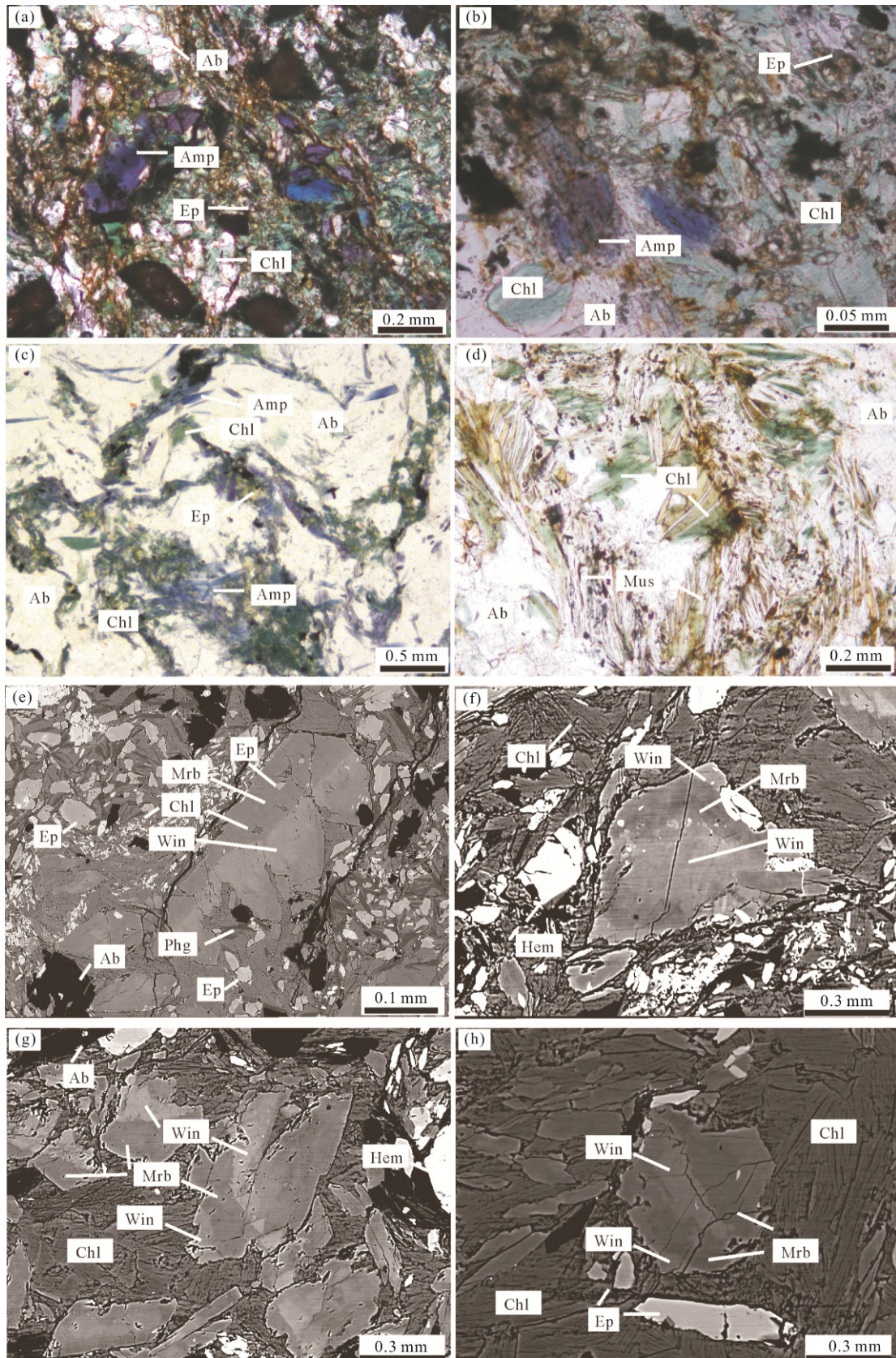
Figure 2. Photomicrographs and Back-scattered electron images of the Toudaoqiao blueschist. (a) Mineral compositions of Sample TD13. Some amphiboles are optical zoned. (b) Mineral compositions of Sample TD7. Some amphiboles are optical zoned. (c) Mineral compositions of Sample TD9. (d) Mineral compositions of Sample TD6. (e) Zoned amphibole coexisting with epidote, phengite, chlorite, albite and hematite, the winchite core has inclusions of chlorite and epidote (TD13); (f), (g) and (h) Zoned amphibole with winchite core, magnesioriebeckite/glaucophane rim and winchite outermost rim (TD13). Abbreviations: Amp. amphibole; Ab. albite; Chl. chlorite; Ep. epidote; Mus. muscovite; Mrb. magnesioriebeckite; Win. winchite; Phg. phengite; Hem. hematite.

Table 1   Microprobe analyses of major minerals from the Toudaoqiao blueschists and pelitic schist

	Amp												
	TD13								Outermost rim	TD9			
	Matrix				Core		Rim			Matrix			
SiO_2 (wt.%)	52.25	53.88	53.81	54.94	53.44	53.39	55.3	53.85	53.68	53.62	56.99	55.46	54.51
TiO_2	0.03	0.13	0.14	0	0.07	0.05	0.05	0	0.04	0.05	0.07	0.07	0.08
Al_2O_3	2.74	2.72	3.48	5.74	2.58	2.58	3.29	3.11	1.98	2.56	4.49	4.69	3.37
Cr_2O_3	0.01	0.01	0.03	0	0	0	0	0	0	0	0	0.08	0.04
FeO	20.46	22.15	21.72	18.24	22.94	21.92	20.87	23.35	19.02	20.23	19.07	18.63	20.83
MnO	0.23	0.23	0.21	0.28	0.27	0.26	0.26	0.18	0.37	0.26	0.24	0.27	0.29
MgO	10.42	8.78	8.32	8.46	8.91	9.36	9.03	7.41	11.28	9.86	7.79	8.64	8.97
CaO	5.76	2.69	1.93	1.06	4.44	4.21	1.97	1.27	5.31	3.59	0.62	0.49	1.27
Na_2O	4.12	5.71	6.2	6.75	4.77	4.9	6.26	6.54	4.17	5.48	6.55	7.45	6.98
K_2O	0.14	0.09	0.06	0.05	0.11	0.11	0.07	0.05	0.09	0.07	0.06	0.05	0.05
Total	96.16	96.39	95.89	95.52	97.53	96.77	97.09	95.76	95.94	95.71	95.88	95.82	96.38
O=	23	23	23	23	23	23	23	23	23	23	23	23	23
Si (apfu)	7.688	7.871	7.88	7.953	7.785	7.802	7.957	7.934	7.834	7.875	8.223	8.03	7.908
Ti	0.004	0.014	0.016	0	0.008	0.005	0.005	0	0.005	0.006	0.007	0.008	0.009
Al	0.475	0.467	0.6	0.979	0.443	0.443	0.558	0.54	0.341	0.442	0.763	0.8	0.576
Cr	0.001	0.001	0.003	0	0	0	0	0	0	0	0	0.009	0.004
Fe^{3+}	1.123	1.286	1.228	0.881	1.216	1.215	1.154	1.315	1.128	1.093	0.741	0.865	1.222
Fe^{2+}	1.394	1.419	1.433	1.327	1.579	1.463	1.357	1.561	1.193	1.391	1.56	1.391	1.306
Mn	0.029	0.028	0.026	0.034	0.033	0.032	0.032	0.023	0.045	0.033	0.03	0.033	0.036
Mg	2.286	1.913	1.816	1.825	1.935	2.039	1.937	1.627	2.455	2.159	1.676	1.864	1.94
Ca	0.908	0.421	0.303	0.164	0.693	0.66	0.303	0.2	0.83	0.565	0.096	0.075	0.197
Na	1.175	1.618	1.761	1.894	1.348	1.388	1.746	1.869	1.178	1.559	1.831	2.09	1.962
K	0.026	0.017	0.012	0.01	0.02	0.021	0.012	0.009	0.016	0.012	0.011	0.01	0.009
Total	15.109	15.055	15.076	15.069	15.061	15.068	15.061	15.077	15.024	15.137	14.938	15.175	15.168

|	Phg					Ep				Chl		
	TD13			TD7		TD13		TD9	TD7	TD13		TD9
SiO_2 (wt.%)	51.74	50.4	50.07	51.76	50.03	36.93	35.31	36.59	36.21	26.91	26.2	26.247
TiO_2	0.17	0.14	0.07	0.04	0.18	0.04	0.05	0.07	0.27	0.04	0.01	0.072
Al_2O_3	24.43	24.17	24.43	23.63	24.18	21.45	19.1	21.7	21.17	18.44	17.92	18.681
Cr_2O_3	5.29	6.95	6.09	5.48	6.08	0.05	0	0	0.03	0	0	0.094
FeO	0.11	0.06	0.06	0.02	0.05	14.74	15.68	13.53	14.25	25.22	24.42	23.313
MnO	3.89	3.77	4.1	4.09	4.53	0.25	0.17	0.19	0.22	0.63	0.61	0.762
MgO	0.05	0.03	0.03	0.1	0.07	0	0.03	0.15	0.04	16.74	16.38	16.402
CaO	0.09	0.11	0.13	0.18	0.15	22.12	18.97	22.53	21.9	0.09	0.07	0.141
Na_2O	10.51	10.64	10.34	10.53	10.25	0	0	0.2	0.02	0.08	0.1	0.004
K_2O	0	0	0.01	0.02	0	0.06	0.04	0.03	0.02	0.06	0.03	0.024
Total	96.28	96.26	95.31	95.85	95.52	95.63	89.34	94.99	94.13	88.18	85.73	85.74
O=	22	22	22	22	22	25	25	25	25	28	28	28
Si (apfu)	6.937	6.839	6.824	6.983	6.806	2.991	3.051	2.983	2.98	5.654	5.659	5.631
Ti	0.017	0.014	0.007	0.004	0.018	0.002	0.003	0.004	0.017	0.006	0.001	0.012
Al	3.86	3.865	3.923	3.757	3.877	2.047	1.945	2.085	2.053	4.566	4.561	4.724
Cr	0	0	0	0	0	0.003	0	0	0.002	0	0	0
Fe^{3+}	0.593	0.788	0.694	0.618	0.692	0.998	1.133	0.923	0.981	0	0	0.016
Fe^{2+}	0.012	0.007	0.006	0.002	0.006	0	1	2	3	4.432	4.41	4.183
Mn	0.778	0.763	0.832	0.823	0.919	0.017	0.013	0.013	0.016	0.112	0.111	0.138
Mg	0.007	0.004	0.004	0.014	0.01	0	0.004	0.018	0.005	5.243	5.274	5.246
Ca	0.023	0.029	0.034	0.047	0.04	1.919	1.756	1.968	1.931	0.02	0.016	0.032
Na	1.798	1.842	1.798	1.812	1.779	0	0	0.016	0.001	0.031	0.044	0.002
K	0	0	0.001	0.002	0	0.006	0.004	0.003	0.002	0.015	0.009	0.007
Total	14.026	14.15	14.123	14.063	14.146	7.985	8.909	10.011	10.987	20.08	20.085	19.991
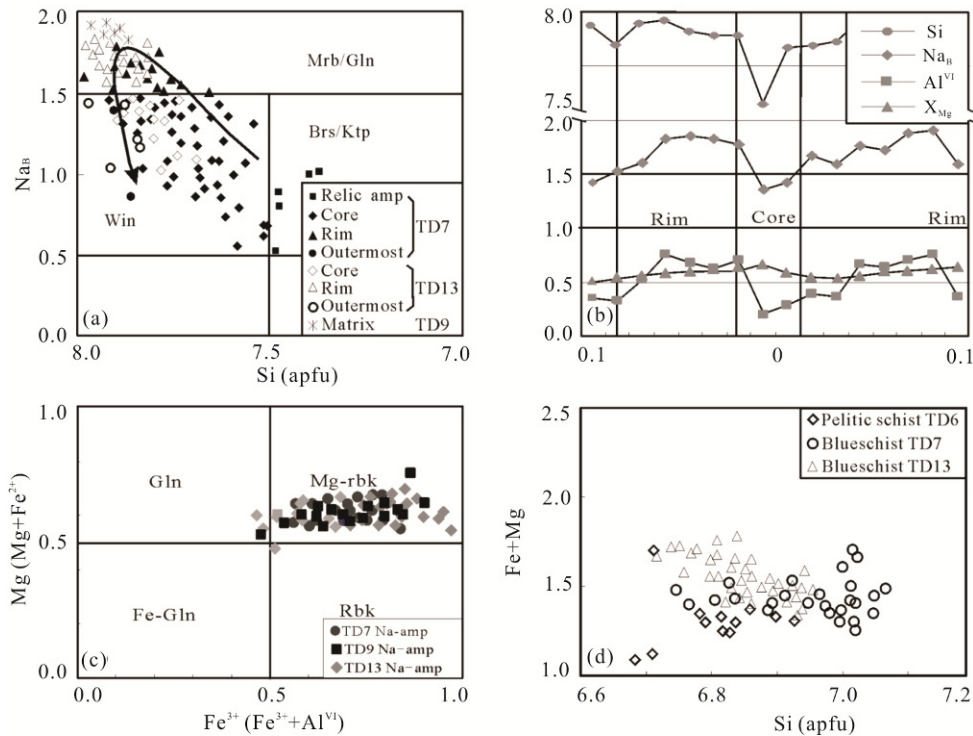
Figure 3. (a) Si vs. Na_B diagram showing chemical compositions of amphibole in the blueschists samples. Arrow shows chemical zoning of amphibole. (b) Chemical variation from core to outermost rim of zoned amphibole in sample TD13. (c) $Fe^{3+}/(Fe^{3+}+Al^{VI})$ vs. $Mg/(Mg+Fe^{2+})$ diagram showing chemical compositions of amphibole in the blueschist samples. (d) Chemical compositions of phengites. Abbreviations: Ktp. kataphorite; Brs. barroisite; Gln. glaucophane; Win. winchite; Mrb. magnesioriebeckite; Rbk. riebeckite.

The prograde metamorphic stage is characterized by winchite, as core of zoned amphiboles, chlorite, epidote, albite, hematite and quartz. The metamorphic conditions of the prograde stage are T>300 °C and P>4 kbar, according to winchite stability field with hematite-bearing basic schist (Fig. 4; Otsuki and Banno, 1990).

The peak metamorphic stage is represented by an equilibrium mineral assemblage of magnesioriebeckite/ glaucophane, epidote, phengite (Si<7.0 apfu), chlorite, albite, hematite and quartz. The chemical compositions of magnesioriebeckite/glaucophane coexisting with epidote and hematite are similar to the sodic-amphibole 6 compositions defined by Evans (1990), that constrain the metamorphic conditions within the epidote-blueschist facies (Fig. 4). The stability field of the magnesioriebeckite/glaucophane and the upper stability limit of albite (Holland, 1983) constrain P-T condition of T=350–600 °C and P=10–13 kbar for the peak stage of the epidote-blueschist facies. Phengites (Si<7.0 apfu) in the matrix suggest an upper pressure limit of <12 kbar for the peak stage (Wei et al., 2009). According to these evidences, the peak metamorphism conditions are T=350–400 °C, P=10–12 kbar.

The retrograde metamorphic stage is characterized by winchite as the outermost rim of the zoned amphiboles, suggesting similar mineral assemblage with the prograde metamorphic stage, also suggesting the similar metamorphic conditions with the prograde metamorphic stage (Fig. 4).

4.2 *P-T* Estimation for the Other Samples

Sample TD7 has similar constituent minerals with sample

TD13, they also have the same *P-T* path. For blueschist sample TD9, the mineral assemblage of peak stage is distinguished as magnesioriebeckite, glaucophane, epidote, chlorite, albite, hematite and quartz, suggesting similar peak metamorphic conditions with the other blueschists. Phengites in pelitic schists sample TD6 also show high Si contents (Si<7.0 apfu), which is consistent with the high *P/T* metamorphic conditions of the blueschist.

5 DISCUSSION AND CONCLUSIONS

The peak metamorphic conditions of the blueschist are the epidote-blueschist facies of T=350–400 °C and P=10–12 kbar (Fig. 4). The prograde (winchite to glaucophane) and retrograde (glaucophane to winchite) paths are likely to be the similar trajectory of the hair-pin type. The peak mineral assemblage of the blueschist is well preserved, only very sharp winchite outermost rim occurring during the retrograde stage, these characters are well corresponding to the Franciscan type, indicate the retrogression approximately retraced the prograde (temperature) *P-T* path (Wei, 1994; Ernst, 1988).

The recent geochemistry data indicate that the protolith of Toudaoqiao blueschist was predominantly metabasalts with OIB and N-MORB affinities (Miao et al., 2015; Zhou et al., 2015), which implies that an ancient subduction zone passes through the Toudaoqiao area. This is corresponding to occurrence of tectonic mélange, which extends in a general NE-SW direction, same with blueschist complex (Fig. 1c). Although there is no typical ophiolites have been reported in this area, the Xinlin Ophiolite has been recognized in the east part of the

Ergun Block for a long time, which is also along the Xinlin-Xiguitu suture (Fig. 1b). Li (1991) has first described the Xinlin ophiolite represents a typical upper mantle-oceanic crust succession. Geochemical data indicate the origin basalts are MORB. The age of ophiolite were reported as 570 Ma. These evidences suggest that the Xinlin-Xiguitu suture was most likely the suture zone between the Ergun and the Xing'an blocks.
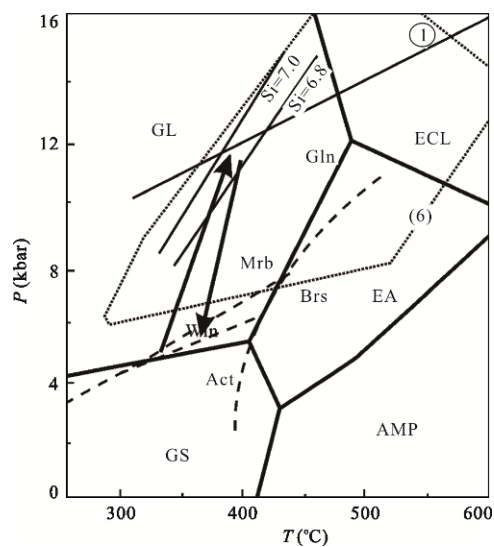

Figure 4. Metamorphic *P-T* history of the blueschists. The boundaries of the metamorphic facies are after Takasu (1989). Broken lines show the stability fields of actinolite, winchite, magnesioriebeckite, glaucophane and barroisite (Otsuki and Banno, 1990). The dotted line (6) is the stability field of sodic-amphibole 6 (Evans, 1990). The isopleths of Si in phengite are referred from (Wei et al., 2009). Reaction 1: albite. jadeite quartz (Holland, 1983). Abbreviations: ECL. eclogite facies; GL. glaucophane schist facies; EA. epidote-amphibolite facies; AMP. amphibolite facies; GS. greenschist facies; Act. actinolite.

The recent geochronological data review the protoliths of the Toudaoqiao blueschist with age of about 510 Ma and syn-collision granitic dike with age of 490 Ma (Miao et al., 2015; Zhou et al., 2015). The Tahe granite, located in the southeastern margin of the Ergun Block, with 490 Ma post-orogenic age, which is consistent with the age of the granitic dike in Toudaoqiao area. It indicates that the collision has occurred at least 490 Ma ago (Ge et al., 2007b; 2005). Besides, both of Ergun and Xing'an blocks have Cambrian or Neoproterozoic meta-igneous rock, which were correlated to the active continental margin. The geochronology information can constrain the maximum age of the collision time between the two blocks (Miao et al., 2007). In summary, the geochronological data from the blueschist, ophiolite and post-orogenic granite record that the oceanic crust between the two blocks was formed at c. 570 Ma, followed by subduction, collision and related metamorphism and magmatism during the period c. 510–490 Ma.

Similar tectonic processes as closure of a paleo-ocean and subsequent continent-continent collision took place among the microcontinents along the southeastern segment of the CAOB (Miao et al., 2007; Xiao et al., 2003; Buchan et al., 2002).

These microcontinents collided with the Siberian Craton along the Mongol-Okhstk belt (Zorin, 1999; Muller et al., 1991). At present, researchers (Badarch et al., 2002; Salnikova et al., 2001; Sal'nikova et al., 1998) suggest that the Ergun Block is connected to the Central Mongolian and Tuvino blocks, and they found that it underwent an orogenic metamorphic event at 536±6 Ma, with emplacement of a series of 490 Ma granitic plutons during the post-orogenic stage, coeval with the emplacement of the Early Paleozoic Tahe pluton and other post-orogenic granitoids in Ergun Block.

REFERENCES CITED

Badarch, G., Cunningham, W. D., Windley, B. F., et al., 2002. A New Terrane Subdivision for Mongolia: Implication for the Phanerozoic Crustal Growth of Central. Asia. *Journal of Asian Earth Science*, 21(1): 87–110

Buchan, C., Pfäjder, J., Kröner, A., et al., 2002. Timing of Accretion and Collisional Deformation in the Central Asian Orogenic Belt: Implicaitons of Granite Geochronology in the Bayankhongor Ophiolite Zone. *Chemical Geology*, 192(1–2): 23–45

Chen, L., Sun, J. G., Chen, X. S., et al., 2009. Zircon LA-ICP-MS U-Pb Dating of Granite from the Yinchengzi Gold Deposit Area in the Eastern Zhang Guang Cailing Area and Its Geological Significance. *Acta Geologica Sinica*, 83: 1327–1334

Ernst, W. G., 1988. Tectonic History of Subduction Zones Inferred from Retrograde Blueschist P-T Paths. *Geology*, 16(12): 1081–1084

Evans, B. W., 1990. Phase Relations of Epidote-Blueschists. *Lithos*, 25(1–3): 3–23

Gao, F. H., Xu, W. L., Yang, D. B., et al., 2007. LA-ICP-MS Zircon U-Pb Dating from Granitoids in Southern Basement of Songliao Basin: Constraints on Ages of the Basin Basement. *Science in China D*: Earth Science, 50: 995–1004

Ge, W. C., Wu, F. Y., Zhou, C. Y., et al., 2005. Emplacement Age of the Tahe Granite and Its Constraints on the Tectonic Nature of the Erguna Block in the Northern Part of the Da Hinggan Range. *Chinese Science Bulletin*, 50(7): 2097–2105

Ge, W. C., Sui, Z. M., Wu, F. Y., et al., 2007a. Hf Isotopic Characteristics and Their Implications of the Early Paleozoic Granites in the Northern Da Hinggan Mts., Northeastern China. *Acta Petrologica Sinica*, 23(2): 423–440 (in Chinese with English Abstract)

Ge, W. C., Wu, F. Y., Zhou, C. Y., et al., 2007b. Porphyry Cu-Mo Deposits in the Eastern Xing'an-Mongolian Orogenic Belt: Mineralization Ages and Their Geodynamic Implications. *Chinese Science Bulletin*, 52(24): 3416–3427

Heilongjiang Bureau of Geology and Mineral Resources (HBGMR), 1981. Explanation of the Geological Map of the Taerqi Sheet with a 1 : 200 000 Scale. 204–207 (in Chinese)

Heilongjiang Bureau of Geology and Mineral Resources (HBGMR), 1993. Regional Geology of Heilongjiang Province. Geological Publishing House, Beijing. 527 (in Chinese)

Holland., T, J. B., 1983. Experimental Determination of the Activities in Disordered and Short-Range Ordered Jadeitic Pyroxene. *Contributions to Mineralogy and Petrology*, 82(2): 214–220

Kretz, R., 1983. Symbols for Rock-Forming Minerals. *American Mineralogist*, 68(1): 277–279

Leake, B. E., Woolley, A. R., Arps, C. E. S., et al., 1997. Nomenclature of Amphiboles: Report of the Subcommittee on Amphiboles of the International Mineralogical Association, Commission on New Minerals and Mineral Names. *Mineralogical Magazine*, 61(405): 295–321

Li, R. S., 1991. Xinlin Ophiolite. *Heilongjiang Geology*, 2(1): 19–32 (in Chinese with English Abstract)

Maruyama, S., Liou, J., Terabayashi, M., 1996. Blueschists and Eclogites of the World and Their Exhumation. *International Geology Review*, 38(6): 485–594

Miao, L. C., Fan, W. M., Zhang, F. Q., et al., 2003. Zircon SHRIMP Geochronology of the Xinkailing-Kele Complex in the Northwestern Lesser Xing'an Range, and Its Geological Implications. *Chinese Science Bulletin*, 49(2): 201–209

Miao, L. C., Liu, D. Y., Zhang, F. Q., 2007. Zircon SHRIMP U-Pb Ages of the "Xinghuadukou Group" in Hanjiayuanzi and Xinlin Areas and the "Zhalantun Group" in Inner Mongolia, Da Hinggan Mountains. *Chinese Science Bulletin*, 52(8): 1112–1124

Miao, L. C., Zhang, F. C., Jiao, S. J., 2015. Age, Protoliths and Tectonic Implications of the Toudaoqiao Blueschists, Inner Mongolia, China. *Journal of Asian Earth Sciences*, 105: 360–373

Miyashiro, A., 1961. Evolution of Metamorphic Belts. *Journal of Petrology*, 2(3): 277–311

Mo, Y. C., 1980. The Petrological Description of the Toudaoqiao Blueschists. *Heilongjiang Geology*, 2 (in Chinese)

Muller, J. F., Rogers, J. J. W., Jin, Y. G., et al., 1991. Late Carboniferous to Permian Sedimentation in Inner Mongolia, China, and Tectonic Relationships between North China and Siberia. *Journal of Geology*, 99(3): 251–263

Otsuki, M., Banno, S., 1990. Prograde and Retrograde Metamorphism of Hematite-Bearing Basic Schists in the Sanbagawa Belt in Central Shikoku. *Journal of Metamorphic Geology*, 8(4): 425–439

Peng, Y. J., Ji, C. H., Xin, Y. L., 2002. Petrology and Geochronology of the Paleo-Jilin-Heilongjiang Orogenic Belt in the Adjacent Areas of China, Russion and Korea. *Geology and Resources*, 11(2): 65–75

Sal'nikova, E. B., Sergeev, S. A., Kotov, A. B., et al., 1998. U-Pb Zircon Dating of Granulite Metamorphism in the Sludyanskiy Complex, Eastern Siberia. *Gondwana Research*, 1(2): 195–205

Sal'nikova, E. B., Kozakov, I. K., Kotov, A. B., et al., 2001. Age of Palaeozoic Granites and Metamorphism in the Tuvino-Mongolian Massif of the Central Asian Mobile Belt: Loss of a Precambrian Microcontinent. *Precambrian Research*, 110(1): 143–164

Sengör, A. M. C., Natal'in, B. A., Burtman, V. S., 1993. Evolution of the Altaid Tectonic Collage and Palaeozoic Crustal Growth in Eurasia. *Nature*, 364(6435): 299–307

Takasu, A., 1989. P-T Histories of Peridotite and Amphibolite Tectonic Blocks in the Sanbagawa Metamorphic Belt, Japan. In: Daly, J. S., Cliff, R. A. Yardley, B. W. D. eds., Evolution of Metamorphic Belts. *Geological Society Special Publication*. 43(1): 533–538

Wang, Y., Zhang, F. Q., Zhang, D. W., et al., 2006. Zircon SHRIMP U-Pb Dating of Meta-Diorite from the Basement of the Songliao Basin and Its Geo-

logical Significance. *Chinese Science Bulletin*, 51(15): 1877–1883

Wei, C. J., 1994. Progress in the Study of Blueschists and Related High Pressure Metamorphic Belts. *Earth Science Frontiers*, 1(1–2): 140–144 (in Chinese with English Abstract)

Wei, C. J., Su, X. L., Li, Y. J., 2009. A New Interpretation of the Conventional Thermobarometry in Eclogite: Evidence from the Calc Ulated PT Pseudosections. *Acta Petrologica Sinica*, 25(09): 2078–2088

Wilde, S. A., Dorsett, B. H., Liu, J. L., 1997. The Identification of A Late Pan-African Granulite Facies Event in Northeastern China: SHRIMP U-Pb Zircon Dating of the Mashan Group at Liu Mao, Heilongjiang Province, China. Proceedings of the 30th IGC: Precambrian Geology and Metamorphic Petrology, VSP International. Science Publishers, Amsterdam. 17, 59–74

Wilde, S. A., Wu, F. Y., Zhang, X. Z., 2003. Late Pan-African Magmatism in Northeastern China: SHRIMP U-Pb Zircon Evidence for Igneous Ages from the Mashan Complex. *Precambrian Research*, 122(1–4): 311–327

Wu, F. Y., Sun, D. Y., Li, H. M. et al., 2001. The Nature of Basement beneath the Songliao Basin in NE China: Geochemical and Isotopic Constraints. *Physics and Chemistry of the Earth* (*Part A*), 26(9): 793–803

Wu, F. Y., Sun, D. Y., Ge, W. C., et al., 2011. Geochronology of the Phanerozoic Granitoids in Northeastern China. *Journal of Asian Earth Sciences*, 41(1): 1–30

Wu, F. Y., Zhao, G. C., Sun, D. Y., et al., 2007. The Hulan Group: Its Role in the Evolution of the Central Asian Orogenic Belt of NE China. *Journal of Asian Earth Sciences*, 30(3–4): 542–556

Xiao, W. J., Windley, B., Hao, J., et al., 2003. Accretion Leading to Collision and the Permian Solonker Suture, Inner Mongolia, China: Termination of the Central Asian Orogenic Belt. *Tectonics*, 22(6): 1–20

Xiao, W. J., Windley, B. F., Huang, B. C., et al., 2009. End Permian to Mid-Triassic Termination of the Southern Central Asian Orogenic Belt. *International Journal of Earth Sciences*, 98: 1189–1217

Ye, H. W., Zhang, X. Z., Zhou, Y. W., 1994. The Texture and Evolution of Manzhouli-Suifenhe Lithosphere-Study Based on Features of Blueschist and Ophiolites. In Geological Studies of Lithospheric Structure and Evolution of Manzhouli-Suifenhe Geotransect, China In: M-SGT Geology Group ed.. Seismic Press, Beijing. 73–83 (in Chinese)

Zhang, J. H., Ge, W. C., Wu, F. Y., et al., 2008. Large-Scale Early Cretaceous Volcanic Events in the Northern Great Xing'an Range, Northeastern China. *Lithos*, 102(1–2): 138–157

Zhang, M. S., Peng, X. D., Sun, X. M., 1998. The Paleozoic Tectonic Geographical Pattern of Northeast China. *Liaoning Geology*, 2: 91–96 (in Chinese with English Abstract)

Zhao, S., Xu, W. L., Tang, J., et al., 2016. Neoproterozoic Magmatic Events and Tectonic Attribution of the Erguna Massif: Constraints from Geochronological, Geochemical and Hf Isotopic Data of Intrusive Rocks. *Earth Science—Journal of China University of Geosciences*, 41(11):1803–1829

Zhou, J. B., Wilde, S. A., Zhang, X. Z., 2011. Early Paleozoic Metamorphic Rocks of the Erguna Block in the Great Xing'an Range, NE China: Evidence for the Timing of Magmatic and Metamorphic Events and Their Tectonic Implications. *Tectonophysics*, 499(1–4): 105–117

Zhou, J. B., Wang, B., Wilde, S. A., et al., 2015. Geochemistry and U-Pb Zircon Dating of the Toudaoqiao Blueschists in the Great Xing'an Range, Northeast China, and Tectonic Implications. *Journal of Asian Earth Sciences*, 97: 197–210

Zorin, Y. A., 1999. Geodynamics of the Western Part of the Mongolia-Okhotsk Collisional Belt, Trans-Baikal Region (Russia) and Mongolia. *Tectonophysics*, 306(1): 33–45